Solvent Accessibility of Protein Surfaces by Amide H/^{2}H Exchange MALDI-TOF Mass Spectrometry

Stephanie M. E. Truhlar, Carrie H. Croy, Justin W. Torpey, Julia R. Koeppe, and Elizabeth A. Komives
Department of Chemistry and Biochemistry, University of California-San Diego, La Jolla, California, USA

One advantage of detecting amide H/^{2}H exchange by mass spectrometry instead of NMR is that the more rapidly exchanging surface amides are still detectable. In this study, we present quench-flow amide H/^{2}H exchange experiments to probe how rapidly the surfaces of two different proteins exchange. We compared the amide H/^{2}H exchange behavior of thrombin, a globular protein, and IκBα, a nonglobular protein, to explore any differences in the determinants of amide H/^{2}H exchange rates for each class of protein. The rates of exchange of only a few of the surface amides were as rapid as the "intrinsic" exchange rates measured for amides in unstructured peptides. Most of the surface amides exchanged at a slower rate, despite the fact that they were not seen to be hydrogen bonded to another protein group in the crystal structure. To elucidate the influence of the surface environment on amide H/^{2}H exchange, we compared exchange data with the number of amides participating in hydrogen bonds with other protein groups and with the solvent accessible surface area. The best correlation with amide H/^{2}H exchange was found with the total solvent accessible surface area, including side chains. In the case of the globular protein, the correlation was modest, whereas it was well correlated for the nonglobular protein. The nonglobular protein also showed a correlation between amide exchange and hydrogen bonding. These data suggest that other factors, such as complex dynamic behavior and surface burial, may alter the expected exchange rates in globular proteins more than in nonglobular proteins where all of the residues are near the surface. (J Am Soc Mass Spectrom 2006, 17, 1490–1497) © 2006 American Society for Mass Spectrometry

Amide H/^{2}H exchange experiments provide unique insights into protein conformation and flexibility. The use of mass spectrometry to detect amide H/^{2}H exchange has advantages and disadvantages. The experiment is usually performed in such a way that the protein is allowed to exchange in deuterated buffer, then the exchange reaction is quenched, the protein is digested under quench conditions by pepsin, and finally the pepsin digest is analyzed by mass spectrometry [1]. The main disadvantage of most current mass spectrometric methods is that it is only possible to obtain regio-specific information because of uncertainties regarding scrambling when CID is used to obtain amide-specific information [2, 3]. The primary advantage of using mass spectrometry to detect the exchanged amides is that the experimental measurement is rapid enough to detect even the most rapidly exchanging amides [4, 5]. This is not true for NMR H/^{2}H exchange measurements where detection depends on the time-frame of the exchange and often the rapidly exchanging amides are not detected [6]. Other advantages of using mass spectrometry to detect amide H/^{2}H exchange include the ability to detect two states of a protein, since the states are seen as two populations rather than an average, as is the case in the NMR experiment, and the ease of identifying specific amides by peptide sequencing compared with having to assign the NMR spectrum.

When the goal of the experiment is to understand the folding of a protein from the denatured state to the fully-folded state, either mass spectrometry or NMR can be used to equal advantage because the protein folding reaction is accompanied by huge differences, often as much as 10^7, in the rates of exchange between the unfolded state and the folded state, as was shown in the pioneering work of Englander's group [7]. However, when the goal of the experiment is to understand what happens to the protein surface during a protein–protein interaction, or changes that occur upon ligand binding, mass spectrometry is often the method of choice. In these cases, the differences in amide exchange

Published online August 24, 2006
Address reprint requests to Dr. E. A. Komives, Department of Chemistry and Biochemistry, University of California-San Diego, La Jolla, CA 92093-0378, USA. E-mail: ekomives@ucsd.edu

1044-0305/06/$32.00
doi:10.1016/j.jasms.2006.07.023

Received March 31, 2006
Revised July 24, 2006
Accepted July 25, 2006

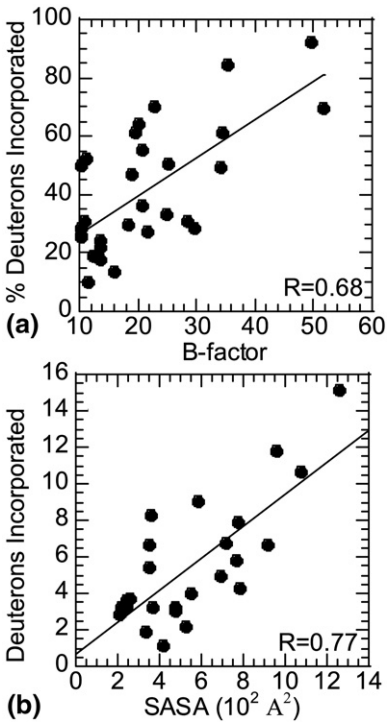

Figure 1. (**a**) The correlation between the percent of amides H/^{2}H exchanged after 2 min of on-exchange in the methylesterase CheB and the average crystallographic B-factor across the same peptide region (from PDB accession number 1A2O) [24] was 0.68 (these results were presented previously) [8]. The percent exchanged is used in this correlation because the total number of amides exchanged is dependent on the length of each peptide, whereas the percent exchanged is length-independent, as is the average B-factor across the peptide. (**b**) The correlation between number of amides exchanged in the methylesterase CheB in 10 min and the solvent accessible surface area per peptide (SASA) calculated using Getarea 1.1 [29] was somewhat higher (R = 0.77). Since the SASA is length-dependent, in this case, the correlation should be between the SASA and the total number of deuterons per peptide.

are much more subtle, as the amide may not be hydrogen bonded to a protein group in either state, but rather the environment around the amide that affects its solvent accessibility changes.

We previously published amide H/^{2}H exchange experiments to probe the solvent accessibility changes occurring in the chemotaxis protein methylesterase CheB upon phosphorylation [8]. In this study, the data were shown to correlate with the crystallographic B-factors with a correlation coefficient of 0.68 (Figure 1a). Others have shown similar correlations with solvent accessible surface area (SASA) [9], and we find that for CheB, amide H/^{2}H exchange correlates even better with this parameter than with the B-factors (Figure 1b). This is likely because the crystallographic B-factor, which tends to be interpreted in terms of protein flexibility, also depends on crystal packing forces. Theoretical studies show that the density of contacts are well-correlated with H/^{2}H protection factors, B-factors and SASA [10, 11]. This implies that all of the experimental measurements are inter-related by the density of contacts and, as such, should all correlate to some degree. It is important to note that all of the positive correlations of amide exchange with SASA are for exchange data obtained from mass spectrometry measurements, which sample all of the time regimes of exchange. Attempts to correlate amide exchange measured by NMR, which only detects amides with half-lives longer than 15 min, with such structural parameters were unsuccessful [12].

While most proteins fold to a compact, globular native structure with a buried hydrophobic core, there are many nonglobular repeat proteins that are stabilized by intra-repeat interactions and lack a well-buried core [13]. For globular proteins, amide exchange is typically very slow in the core of the protein, where amides are hydrogen bonded to other protein groups and excluded from solvent. Near the surface of the protein, the amides exchange more rapidly and there is a continuum of rates of exchange between the core and the surface [14, 15]. The rates of exchange are determined by a complex set of factors including the hydrogen bonding state of the amide, the protein flexibility, and the distance of the amide from the surface. However, for nonglobular proteins, the entire protein is essentially near the surface, reducing the number of factors that influence exchange to hydrogen-bonding and flexibility. Thus, amide exchange studies of these proteins will enable a better understanding of the influences of protein conformation and dynamics on amide H/^{2}H exchange rates.

In this paper, we present data from quench-flow amide exchange experiments that probe the most rapidly exchanging amides on the surface of two proteins, thrombin, a typical globular protein (Figure 2a), and IκBα, a nonglobular ankyrin repeat protein (Figure 2b). The influence of the density of contacts and the envi-

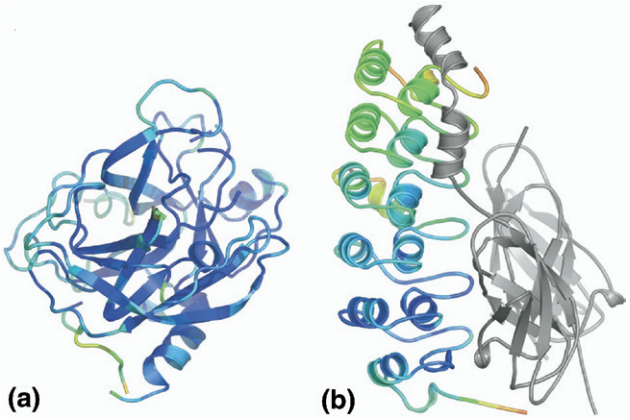

Figure 2. Structures of (**a**) the globular protein, thrombin (PDB accession number 1PPB) [26] and (**b**) the nonglobular protein, IκBα (PDB accession number 1NFI) [25] colored according to the crystallographic B-factors. The structure of IκBα was determined in complex with NF-κB (colored grey). Figures were prepared using PyMOL version 0.97 available at (http://pymol.sourceforge.net/) (DeLano Scientific, South San Francisco, CA) [32].

ronment of the surface of a protein on amide H/^{2}H exchange was investigated. We found that for surface loops, the number of amides exchanging at relatively short times was most closely related to the total solvent accessible surface area of the loop.

Experimental

Proteins

Bovine prothrombin was purified from a barium citrate eluate (prepared from bovine plasma) according to previously published methods [16]. Bovine thrombin was obtained from purified bovine prothrombin by activation with *Echis carinatus* venom, as described previously [5, 16]. The specific activity of these pooled fractions was typically 4000 U/mg [17]. Bovine thrombin was buffer exchanged into 25 mM KH_2PO_4 pH 6.5, 50 mM NaCl, concentrated by partial lyophilization to ~3 mg/mL, and stored as 5 μL aliquots (750 pmol/tube) at −80 °C until use. Control experiments were performed with lyophilized bovine thrombin to verify that there was no difference in deuterium incorporation or pepsin digestion in lyophilized samples compared to non-lyophilized samples.

Human IκB$\alpha_{67\text{-}287}$ was expressed in *Escherichia coli* BL21 (DE3) [18] and purified as previously described [19]. Protein concentrations were quantified spectrophotometrically at 280 nm, as described previously [20], and by dye binding using reducing agent compatible BCA assay (Pierce Biotechnology).

Quench-Flow H/^{2}H Exchange

Experiments to measure amide exchange in bovine thrombin by quench-flow were carried out using a Kin-Tek RQF-3 flow quench apparatus (Kin-Tek Corporation, Clarence, PA). A schematic of the instrument is shown in Figure 3. A 5 mL drive syringe for Sample A (hereafter referred to as the D_2O syringe) and a 0.5 mL drive syringe for Sample B (hereafter referred to as the sample syringe) were installed to accomplish the ~tenfold dilution required for H/^{2}H exchange experiments. Similarly, sample loop A was replaced with a loop that holds ten times the volume of sample loop B. After modifications were completed, the loops were calibrated according to the manufacturer's instructions. Before each experiment, the instrument was thoroughly cleaned with a nonfoaming detergent and washed exhaustively with MilliQ water (Millipore Corporation, Billerica, MA). The D_2O syringe and syringe line were loaded with D_2O from each respective loading port. The sample syringe was loaded with sample buffer, but the sample line, the delay line, and the exit line were completely dry before loading the sample line. The protein sample (45 μL) was loaded via micropipetter into the sample line (B) until the sample meniscus just reached the metal connection to the eight-way valve. The sample valve was switched to the fire position

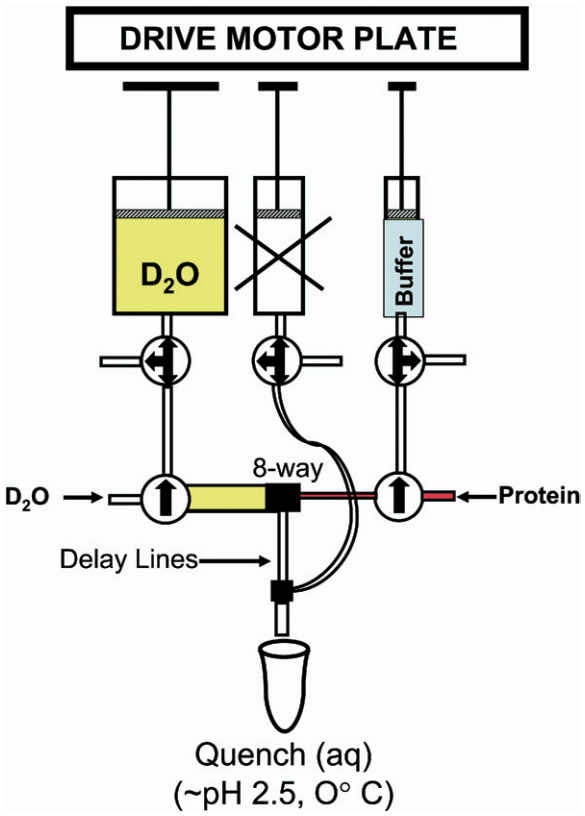

Figure 3. A schematic diagram for the Kintek QF-3 instrument showing the D_2O in yellow, the protein sample in red, and the sample buffer in cyan. The volumes of loops 1–7 are 16.4 μL (max time 13.3 ms), 35.6, 62.9, 98.8, 135.9, 180.39, 333.39 μL (max time 270.7 ms), respectively. The revolution loop volume is 461.89 μL, and the exit line volume is 117.69 μL.

immediately. Although only 19 μL from the sample line is delivered per reaction, the set-up requires a total of 45 μL be loaded into the instrument. The eight-way valve was fitted with different sized delay lines depending on the experiment time with the largest loop holding 0.334 ml (the entire sample volume). A quench-vial with a closed lid through which a hole had been punched, was placed in a container of ice with the exit line inserted in the hole to prevent splashing. The third "quench" syringe was not used because we needed to maintain the exact same volume of final quenched solution. Instead, the quench vial contained an appropriate volume of TFA solution to accomplish the quench. The exit line volume/distance was included in all calculations of deuteration times.

Deuteration was initiated when 19 μl of a 122 μM bovine thrombin solution in 330 mM KH_2PO_4, pH 6.5, 660 mM NaCl (2.3 nmol) was diluted 13.8-fold into D_2O (Cambridge Isotope Laboratories, Andover, MA, 203 μl) at room temperature for 0.05, 0.5, 5, 50, and 120 s using the Kin-Tek RQF-3. The quench vial contained 1190 μl of a quench buffer composed of water and 2% TFA, making the final solution ~ 0.1% TFA, pH 2.2 containing 0.7 pmol/μl in bovine thrombin. For IκBα

(130 μM), the experimental set-up was the same as for the bovine thrombin but the buffer was 50 mM Tris, 150 mM NaCl, 1 mM DTT (pH 7.7), and the deuteration periods were 0.1, 2.5, 5, 10, 20, 30, 60, 120, 300 s.

A sample (150 μL) of the quenched protein was immediately digested with immobilized pepsin (25 μL, Pierce Biotechnology, Rockford, IL) for 10 min (for bovine thrombin) and 1 min or 5 min (for IκBα) on ice. The digest was divided into several fractions, rapidly frozen in liquid N_2, and stored at −80 °C. All exchange reactions were performed in triplicate.

Amide H/^{2}H Exchange Under Nonquench-Flow Conditions

The exchange reaction for the IκBα protein was initiated by diluting 2 μL of 130 μM IκBα, in 50 mM Tris, 150 mM NaCl, 1 mM DTT (pH 7.5), ten-fold into D_2O. The reaction proceeded for 0, 0.5, 1, 2, or 5 min at ambient temperature, and then the reaction was quenched by six-fold dilution with 0.1% TFA at 0 °C (sample pH = 2.2). The reaction (120 μL) was immediately transferred to 25 μL of immobilized pepsin (Pierce Biotechnology), digestion proceeded for 1 min or 5 min, and 10 μL aliquots of each digestion were immediately frozen in liquid N_2, and stored at −80 °C until analysis. Exchange reactions were performed in triplicate.

Mass Spectrometry

Matrix-assisted laser desorption ionization time-of-flight (MALDI-TOF) mass spectra were acquired on a Voyager DE-STR instrument (Applied Biosystems) as previously described [21]. The matrix used was 5.0 mg/ml α-cyano-4-hydroxycinnamic acid (Sigma-Aldrich) dissolved in a solution containing a 1:1:1 mixture of acetonitrile, ethanol, and 0.1% TFA. The pH of the matrix was adjusted to pH 2.2 using 2% TFA. The matrix solution was chilled on ice for at least 60 min before use and the MALDI-target plates were chilled overnight at 4 °C. All samples were analyzed by MALDI-TOF mass spectrometry one at a time. Samples were rapidly thawed, mixed with cold matrix, spotted on a prechilled MALDI target plate, and dried under vacuum [21]. The mass spectra were analyzed to determine the average number of deuterons present in each peptic peptide. The number of deuterons incorporated into each peptide was quantified by subtracting the centroid of the undeuterated control from the centroid of the isotopic peak cluster for the deuterated sample. All values reported represent only the deuterons exchanged onto the backbone amide-hydrogen (NH) positions. The residual deuterium content that incorporated into rapidly exchanging side-chain positions was subtracted (4.5% for quenched-flow experiments and 7.5% for IκBα in the nonquenched-flow experiments) were subtracted from the total number of deuterons incorporated, yielding only the backbone deuteration. Finally, data were corrected for back-exchange loss (which ranged from 25 to 45% depending on the time of pepsin digestion) as described previously [19, 22]. Data were fit using an exponential fit in Kaleidagraph (Symantec) as described previously [8].

Peptide Identification

Peptides produced by pepsin cleavage of thrombin were identified previously [5, 23]. IκBα peptic peptides were identified by matrix-assisted laser desorption ionization tandem mass spectrometry (MALDI MS/MS) on a Q-STAR XL hybrid quadrupole time-of-flight mass spectrometer with an orthogonal MALDI source (Applied Biosystems) or a 4800 MALDI tandem time-of-flight mass spectrometer (Applied Biosystems).

Solvent Accessible Surface Area Calculations

Calculations were performed on Protein Data Bank files containing the coordinates of Methylesterase CheB (1A2O), the catalytic subunit of CheB (1CHD) [24], and IκBα$_{70-287}$ from the IκBα - p50/p65 complex, (1NFI) [25]. For IκBα, files were created for each copy found in the asymmetric unit and the subsequent calculations were performed separately for both copies. To control for any differences in the form of thrombin, three different structures were used; D-Phe-Pro-Arg-chloromethylketone-bound human α-thrombin (1PPB) [26], D-Phe-Pro-Arg-chloromethylketone-bound bovine thrombin (1ETS) [27], and S195A human thrombin representing the sodium-free "slow" form (1JOU) [28]. Solvent accessible surface area (SASA) calculations were performed using Getarea (version 1.1) available at http://www.scsb.utmb.edu/cgi-bin/get_a_form.tcl [29], using a radius of 1.4 Å and default atomic radii and atomic solvent parameters.

Results and Discussion

Rates of Exchange in Solvent Accessible Surface Loops of Proteins

On-exchange (deuterium incorporation) experiments probe the solvent accessibility of backbone amides in bovine thrombin, a globular protein (Figure 2a) and the ankyrin repeat domain of IκBα, a nonglobular protein (Figure 2b). Quench-flow methods reveal the number of amides exchanging in the first few hundred milliseconds (Table 1). The incorporation of deuterium over time is seen in the MALDI data from the peptide MH+ 1374.77 from IκBα (Figure 4a). The kinetic plot of exchange into this surface loop is shown in Figure 4b. Experiments were always performed in triplicate, and the error bars are barely discernable because the quench-flow apparatus generates highly reproducible results. Kinetic plots of deuteration of two bovine thrombin surface loops covered by the peptides MH+ 2586.48 (residues 96–116) and MH+ 2162.12 (residues

Table 1. Deuterons incorporated over time into protein surface loops

A. Bovine thrombin						
Peptide MH+	Residues	Amides	0.05 s	0.5 s	5 s	50 s
2586.48	109–129	20	5.28 ± 0.29	8.38 ± 0.12	12.29 ± 0.14	17.76 ± 0.34
2102.12	130–145	14	1.32 ± 0.33	2.27 ± 0.19	3.49 ± 0.06	8.15 ± 0.22
2162.12	184–202	18	3.24 ± 0.30	6.28 ± 0.31	9.99 ± 0.42	11.65 ± 0.35
1165.62	227–235	8	1.73 ± 0.18	2.66 ± 0.35	2.71 ± 0.21	3.47 ± 0.20
B. IκBα						
Peptide MH+	Residues	Amides	0.1 s	2.5 s	5 s	60 s
1761.86	66–80	14	4.83 ± 0.02	6.40 ± 0.19	6.96 ± 0.04	9.53 ± 0.09
1374.77	92–103	11	1.03 ± 0.11	3.15 ± 0.13	3.85 ± 0.17	5.98 ± 0.13
1679.89	104–117	12	1.05 ± 0.19	1.71 ± 0.06	1.82 ± 0.01	1.85 ± 0.07
1054.58	142–150	7	0.73 ± 0.16	0.78 ± 0.07	0.86 ± 0.05	1.13 ± 0.08
1221.66	176–186	10	0.78 ± 0.15	1.96 ± 0.02	2.01 ± 0.07	2.17 ± 0.10
2028.01	201–220	18	2.57 ± 0.12	5.46 ± 0.24	6.72 ± 0.28	10.86 ± 0.13

171–189) are shown in Figure 5a and b. It can be seen from these plots that different surface loops on thrombin became deuterated at different rates and to different extents. Deuteration kinetics for two different surface loops of IκBα, covered by peptides MH+ 1679.89 (residues 104–117) and MH+ 2028.01 (residues 201–220), are shown in Figure 5c and d. Data is presented for other surface loops in Table 1. These data show that for the globular protein, thrombin, the surface loops all exchange to a large extent, whereas not all of the surface loops of the nonglobular IκBα protein exchange readily.

We compared our measured amide H/^{2}H exchange rates with the intrinsic exchange rates reported previously for unstructured peptides. These were reported to average 8.3 s^{-1} at pH 7.5 and 5 °C, with a 5-fold

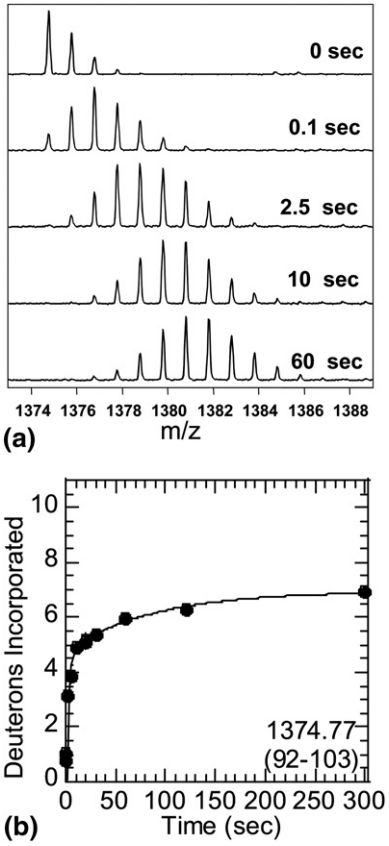

Figure 4. (**a**) Stacked plot of MALDI-TOF mass spectra expanded around the isotopic envelope of the peptide of MH^+ 1374.77 from the peptic digest of IκBα after deuteration for 0, 0.1, 2.5, 10, and 60 s. The higher mass peaks in the envelope prior to deuteration are caused by the presence of naturally occurring isotopes. (**b**) The kinetic plot showing the number of deuterons the peptide of MH^+ 1374.77 incorporates during the various deuteration periods. The maximum of the y-axis represents the total number of amide positions that can be observed for the peptide.

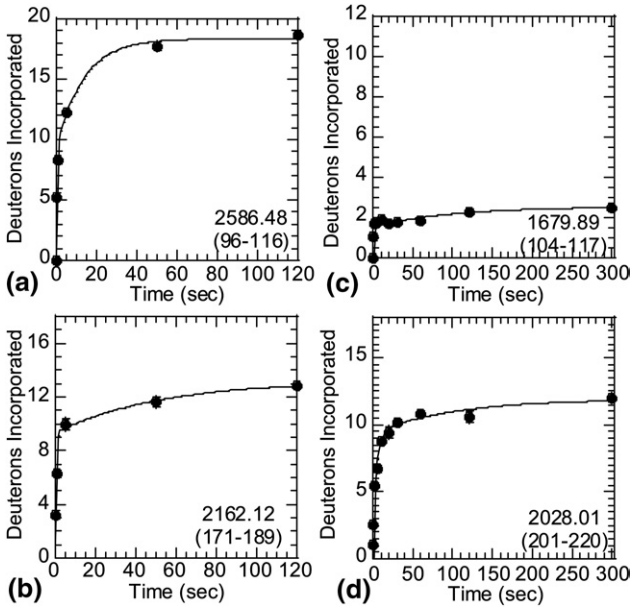

Figure 5. Kinetic plots of deuteration for some surface loop peptides. (**a**) The peptide of MH^+ 2586.48, which is a surface loop (residues 96–116) of bovine thrombin. (**b**) The peptide of MH^+ 2162.12, which is another surface loop (residues 171–189) of bovine thrombin. (**c**) The peptide of MH^+ 1679.89, which is a surface loop (residues 104–117) of IκBα. (**d**) The peptide of MH^+ 2028.01, which is a surface loop (residues 201–220) of IκBα. While most of the surface loops of thrombin exchanged the majority of their amide protons for deuterons, some surface loops of IκBα did not readily exchange.

variation due to side-chain neighbor effects [30]. At 25 °C, the value is expected to increase to 67 s^{-1}. Using special NMR sequences, Gemmecker et al. measured the rates of the rapidly exchanging surface amides by NMR, and they obtain values that range from 50 s^{-1}, at the upper end, to 0.05 s^{-1}, which was the slowest they could measure [15]. Dharmasiri and Smith also measured very rapid exchange rates of >5 s^{-1} on the surfaces of proteins using quench-flow experiments [31]. For thrombin, 5.28 amides exchanged in 50 ms within thrombin residues 109–129 (sequential numbering), covered by the peptide of MH+ 2586.48. This would mean that these amides exchanged at an average rate of 105 s^{-1}, close to that expected from the intrinsic exchange rates of unstructured peptides. It is important to note, however, that the majority of the amides (70%) in this surface loop exchanged at least ten-fold more slowly than the intrinsic rate, although nearly all had exchanged by one min. Thrombin residues 184–202, covered by the peptide of MH+ 2162.12, had 3.24 amides that exchanged in the first 50 msec, corresponding to a rate of 65 s^{-1}, which is again near the intrinsic rate for unstructured peptides. Again, the amides that exchanged at the intrinsic rate represented less than 20% of the amides in this region and, in this case, 43% of the loop had not exchanged by 1 min. Other regions of thrombin had virtually no amides that exchanged at the intrinsic rate (Table 1).

Only the very N-terminus of the ankyrin repeat domain of IκBα, covered by the peptide of MH+ 1761.86, exchanged near the intrinsic rate for unstructured peptides. This region had 4.83 amides exchanged in the first 100 ms, corresponding to a rate of 48 s^{-1}. Some nine of 14 amides in this loop (64%) exchanged more slowly than the intrinsic rate, and four had not exchanged within 1 min. The other surface loops of IκBα had virtually no amides that exchanged at the intrinsic rate, and in some cases less than 20% of the amides had exchanged by one min. Thus, while some amides on the surface of a protein exchange at the rate expected for unstructured peptides, most of the amides exchange much more slowly.

Relationship Between the Exchange of Surface Amides and Their Hydrogen-Bonding Status

To better understand the contribution of hydrogen-bonding to the amide $H/^2H$ exchange rates on protein surfaces, we compared the number of amides that exchanged (after 1 and 2 min deuteration) with the number of amides that were not involved in hydrogen bonds (as seen in the crystal structure) with a protein group. Both thrombin and IκBα have available crystal structures, although the crystal structure of IκBα is only available in complex with NF-κB [25, 26]. Only peptides that showed similar exchange in both free IκBα and IκBα bound to NF-κB were therefore used in the correlations (Truhlar et al., submitted). For the globular protein, thrombin, only a modest correlation was observed, while for the nonglobular protein, IκBα, the correlation was significantly higher (Figure 6a versus 6b). Thus, there appeared to be a difference between globular proteins and nonglobular proteins in terms of how well hydrogen bonding status predicted the extent of amide exchange.

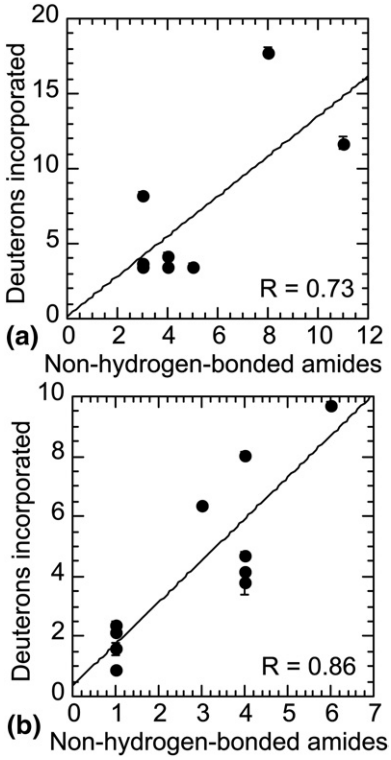

Figure 6. Correlation between the number of amides exchanged in 50 s for each region of thrombin (covered by peptide segments from the pepsin digest) or in 2 min for each region of IκBα and (the total number of amides)–(the number of amides participating in hydrogen-bonds to protein groups) in that segment. The correlation was not as good for (**a**) the globular protein, thrombin (1PPB) [24], as it was for (**b**) the nonglobular protein, IκBα (1NFI) [28].

Correlation Between Solvent Accessible Surface Area and Extent of Amide Exchange

In an effort to understand the factors that control amide exchange at the surfaces of proteins, we compared the number of amides that exchanged with the solvent accessible surface area (SASA) of that region of the protein. It should be noted that the SASA is calculated from the crystal structure and may or may not be the same as the solvent accessibility of a particular region of a protein. This will depend on the breadth of the conformational ensemble of the protein in solution. First, we calculated the total SASA of each region, as well as the SASA for only the protein backbone in these regions. For bovine thrombin, the number of amides exchanged after 50 s, for all peptides derived from bovine thrombin, correlates modestly with both total and backbone SASA, with correlation coefficients of

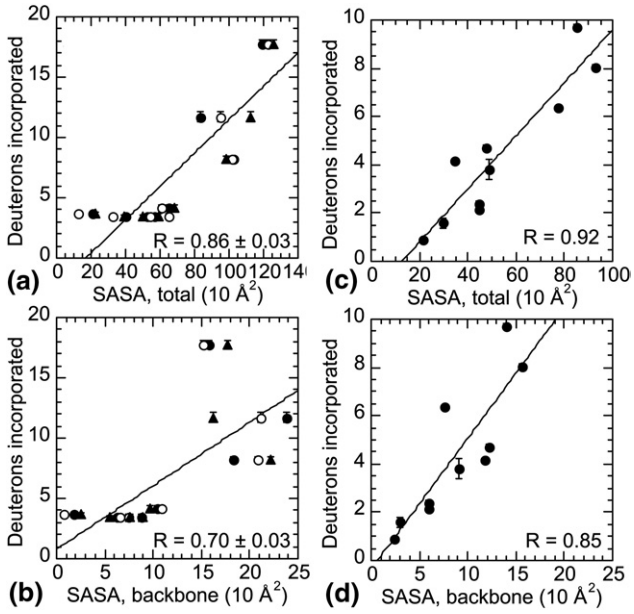

Figure 7. Correlation between the number of amides exchanged in each region covered by peptic peptides from (**a**) and (**b**) the globular protein, thrombin (after 50 s) or (**c**) and (**d**) the nonglobular protein, IκBα (after 2 min) and the solvent accessible surface area (SASA) of that segment. The SASA for each thrombin peptide was calculated using the crystal structures of D-Phe-Pro-Arg chloromethylketone-bound human α-thrombin (1PPB, closed circles) [24], unbound S195A human thrombin (1JOU, open circles) [25], and inhibited bovine thrombin (1ETS, closed triangles) [26]. No significant difference was observed in the correlations with the extent of exchange, regardless of which thrombin structure was used. The SASA for each IκBα peptide was calculated using the IκBα-NF-κB crystal structure (1NFI) [28], from which NF-κB was removed. For both globular and nonglobular proteins, the amide exchange data correlated better with the total SASA, (**a**) and (**c**) than with the backbone SASA, (**b**) and (**d**). Correlations were again much higher for the nonglobular protein, IκBα, than for the globular protein, thrombin.

0.85 and 0.70 (using the human thrombin structure 1PPB); 0.89 and 0.73 (using bovine thrombin structure 1ETS); and 0.84 and 0.67 (using the S195A mutant human thrombin structure 1JOU representing the sodium-free form) (Figure 7a and b). Similar correlations were obtained when data from other time points were used. Since the crystal structure of IκBα is known only in complex with NF-κB, we compared the SASA calculated from the crystal structure with the number of amides exchanged at two min for those peptides from IκBα that showed the same extent of exchange in the free and bound states (Truhlar et al., submitted) (Figure 7c and d). The IκBα amide exchange correlated very well with the total SASA calculated from the crystal structure (0.92). Again, the correlation with the backbone SASA was not as good (0.85).

It is remarkable that the backbone SASA is not as well correlated with amide exchange data as the total SASA, which includes the side chains, since the amide exchange data discussed here reports only on the backbone. This shows that the side chains play a role in protecting otherwise accessible backbone amides from exchange. This has important implications for protein–protein and protein–ligand interactions, since it shows that even binding of a small ligand could perturb the local environment enough to change the amide exchange rate without having any direct contacts, such as protein hydrogen bonds, to the amide proton.

Amide exchange and the total SASA are better correlated for IκBα (0.92), a nonglobular protein, than for either of the globular proteins reported here, the methylesterase CheB (0.77) and thrombin (0.86). For nonglobular proteins, the entire protein is "on the surface" since it lacks a buried hydrophobic core. However, for globular proteins, the buried core is generally protected from exchange; amide exchange in the core of the protein is usually associated with global or local unfolding fluctuations that expose these regions to solvent. Therefore, it seems that the total solvent accessible surface area encompasses the dominant constraints for amide exchange on the surface of proteins, but that for globular proteins, the topological constraints, such as the distance of the amide from the protein surface and the unfolding fluctuations of the protein, are increasingly important determinants of their amide exchange behavior.

Conclusions

We have shown that only a few of the amides in surface loops of proteins, typically some 20%, exchange at the expected intrinsic exchange rates for unstructured peptides, despite the fact that the fraction of amides in these surface loops was highly variable. Amide exchange in thrombin was only modestly correlated with total solvent accessible surface area and with the number of hydrogen bonds to protein groups. The best correlations were obtained for the nonglobular protein, IκBα, where amide exchange was highly correlated with total solvent accessible surface area. These results indicate that for globular proteins, solvent accessible surface area captures much of the structural basis for the extent of amide exchange, however, additional factors superimpose to decrease the correlation. These factors do not seem to be as important in nonglobular proteins.

Acknowledgments

Financial support for this work was provided by NIH RO1-HL070999 to EAK. SMET was supported by a Ruth L. Kirschstein National Research Service Award NIH/NCI T32 CA009523 and a Cancer Research Institute Fellowship.

References

1. Zhang, Z.; Smith, D. L. Determination of Amide Hydrogen Exchange by Mass Spectrometry: A New Tool for Protein Structure Elucidation. *Protein Sci.* **1993,** *2,* 522–531.
2. Jorgensen, T. J.; Gardsvoll, H.; Ploug, M.; Roepstorff, P. Intramolecular Migration of Amide Hydrogens in Protonated Peptides Upon Collisional Activation. *J. Am. Chem. Soc.* **2005,** *127,* 2785–2793.
3. Jorgensen, T. J.; Bache, N.; Roepstorff, P.; Gardsvoll, H.; Ploug, M. Collisional Activation by MALDI Tandem Time-of-Flight Mass Spectrometry Induces Intramolecular Migration of Amide Hydrogens in Protonated Peptides. *Mol. Cell. Proteom.* **2005,** *4,* 1910–1919.

4. Dharmasiri, K.; Smith, D. L. Mass Spectrometric Determination of Isotopic Exchange Rates of Amide Hydrogens Located on the Surfaces of Proteins. *Anal. Chem.* **1996,** *68,* 2340–2344.
5. Croy, C. H.; Koeppe, J. R.; Bergqvist, S.; Komives, E. A. Allosteric Changes in Solvent Accessibility Observed in Thrombin Upon Active Site Occupation. *Biochemistry* **2004,** *43,* 5246–5255.
6. Orban, J.; Alexander, P.; Bryan, P. Hydrogen–Deuterium Exchange in the Free and Immunoglobulin G-Bound Protein G B Domain. *Biochem.* **1994,** *33,* 5702–5710.
7. Englander, S.; Mayne, L. Protein Folding Studied Using Hydrogen-Exchange Labeling and Two-Dimensional NMR. *Annu. Rev. Biophys. Biomol. Struct.* **1992,** *21,* 243–265.
8. Hughes, C. A.; Mandell, J. G.; Anand, G. S.; Stock, A. M.; Komives, E. A. Phosphorylation Causes Subtle Changes in Solvent Accessibility at the Interdomain Interface of Methylesterase CheB. *J. Mol. Biol.* **2001,** *307,* 967–976.
9. Yan, X.; Watson, J.; Ho, P. S.; Deinzer, M. L. Mass Spectrometric Approaches Using Electrospray Ionization Charge States and Hydrogen–Deuterium Exchange for Determining Protein Structures and Their Conformational Changes. *Mol. Cell. Proteom.* **2004,** *3,* 10–23.
10. Shoemaker, B. A.; Wang, J.; Wolynes, P. G. Exploring Structures in Protein Folding Funnels with Free Energy Functional: The Transition State Ensemble. *J. Mol. Biol.* **1999,** *287,* 675–694.
11. Shoemaker, B. A.; Wolynes, P. G. Exploring Structures in Protein Folding Funnels with Free Energy Functionals: The Denatured Ensemble. *J. Mol. Biol.* **1999,** *287,* 657–674.
12. Milne, J. S.; Mayne, L.; Roder, H.; Wand, A. J.; Englander, S. W. Determinants of Protein Hydrogen Exchange Studied in Equine Cytochrome *c*. *Prot. Sci.* **1998,** *7,* 739–745.
13. Mosavi, L. K.; Minor, D. L., Jr.; Peng, Z. Y. Consensus-Derived Structural Determinants of the Ankyrin Repeat Motif. *Proc. Natl. Acad. Sci. U.S.A.* **2002,** *99,* 16029–16034.
14. Jeng, M. F.; Dyson, H. J. Comparison of the Hydrogen-Exchange Behavior of Reduced and Oxidized *Escherichia coli* Thioredoxin. *Biochemistry* **1994,** *34,* 611–619.
15. Gemmecker, G.; Jahnke, W.; Kessler, H. Measurement of Fast Proton Exchange Rates in Isotopically Labeled Compounds. *J. Am. Chem. Soc.* **1993,** *115,* 11620–11621.
16. Ni, F.; Konishi, Y.; Scheraga, H. A. Thrombin-Bound Conformation of the C-Terminal Fragments of Hirudin Determined by Transferred Nuclear Overhauser Effects. *Biochemistry* **1990,** *29,* 4479–4489.
17. Fenton, J. W. Thrombin. *Ann. N.Y. Acad. Sci.* **1986,** *485,* 5–15.
18. Studier, F. W.; Rosenberg, A. H.; Dunn, J. J.; Dubendorff, J. W. Use of T7 RNA Polymerase to Direct Expression of Cloned Genes. *Methods Enzymol.* **1990,** *185,* 60–89.
19. Croy, C. H.; Bergqvist, S.; Huxford, T.; Ghosh, G.; Komives, E. A. Biophysical Characterization of the Free IκBα Ankyrin Repeat Domain in Solution. *Prot. Sci.* **2004,** *13,* 1767–1777.
20. Huxford, T.; Huang, D. B.; Malek, S.; Ghosh, G. The Crystal Structure of the IκBα/NF-κB Complex Reveals Mechanisms of NF-κB Inactivation. *Cell* **1998,** *95,* 759–770.
21. Mandell, J. G.; Falick, A. M.; Komives, E. A. Measurement of Amide Hydrogen Exchange by MALDI-TOF Mass Spectrometry. *Anal. Chem.* **1998,** *70,* 3987–3995.
22. Hughes, C. A.; Mandell, J. G.; Anand, G. S.; Stock, A. M.; Komives, E. A. Phosphorylation Causes Subtle Changes in Solvent Accessibility at the Interdomain Interface of Methylesterase CheB. *J. Mol. Biol.* **2001,** *307,* 967–976.
23. Mandell, J. G.; Falick, A. M.; Komives, E. A. Identification of Protein–Protein Interfaces by Decreased Amide Proton Solvent Accessibility. *Proc. Nat. Acad. Sci. U.S.A.* **1998,** *95,* 14705–14710.
24. Djordjevic, S.; Stock, A. M. Structural Analysis of Bacterial Chemotaxis Proteins: Components of a Dynamic Signaling System. *J. Struct. Biol.* **1998,** *124,* 189–200.
25. Jacobs, M. D.; Harrison, S. C. Structure of an IκBα/NF-κB complex. *Cell* **1998,** *95,* 749–758.
26. Bode, W.; Turk, D.; Karshikov, A. The Refined 1.9-A X-ray Crystal Structure of D-Phe-Pro-Arg Chloromethylketone-Inhibited Human α-Thrombin: Structure Analysis, Overall Structure, Electrostatic Properties, Detailed Active-Site Geometry, and Structure-Function Relationships. *Prot. Sci.* **1992,** *1,* 426–471.
27. Brandstetter, H.; Turk, D.; Hoeffken, H. W.; Grosse, D.; Sturzebecher, J.; Martin, P. D.; Edwards, B. F.; Bode, W. Refined 2.3 A X-ray Crystal Structure of Bovine Thrombin Complexes Formed with the Benzamidine and Arginine-Based Thrombin Inhibitors NAPAP, 4-TAPAP, and MQPA. A Starting Point for Improving Antithrombotics. *J. Mol. Biol.* **1992,** *226,* 1085–1099.
28. Huntington, J. A.; Esmon, C. T. The Molecular Basis of Thrombin Allostery Revealed by a 1.8 A Structure of the "Slow" Form. *Structure* **2003,** *11,* 469–479.
29. Fraczkiewicz, R.; Braun, W. Exact and Efficient Analytical Calculation of the Accessible Surface Areas and Their Gradients for Macromolecules. *J. Comput. Chem.* **1998,** *19,* 319–333.
30. Bai, Y.; Milne, J. S.; Mayne, L.; Englander, S. W. Primary Structure Effects on Peptide Group Hydrogen Exchange. *Proteins* **1993,** *17,* 75–86.
31. Dharmasiri, K.; Smith, D. L. Mass Spectrometric Determination of Isotopic Exchange Rates of Amide Hydrogens Located on the Surfaces of Proteins. *Anal. Chem.* **1996,** *68,* 2340–2344.
32. De Lano, W. L. *The PyMOL User's Manual*; DeLano Scientific: San Carlos, CA, 2002.